

A Shell Model Description of the Decay Out of the Super-Deformed Band of ^{36}Ar

E. Caurier ^a, F. Nowacki ^a and A. Poves ^b

(*a*) IReS, Bât27, IN2P3-CNRS/Université Louis Pasteur BP 28, F-67037 Strasbourg Cedex 2, France

(*b*) Departamento de Física Teórica, C-XI. Universidad Autónoma de Madrid, E-28049, Madrid, Spain

(Dated: June 26, 2018)

Large scale shell model calculations in the valence space spanned by two major oscillator shells (*sd* and *pf*) describe simultaneously the super-deformed excited band of ^{36}Ar and its spherical ground state. We explain the appearance of this super-deformed band at low excitation energy as a consequence of the very large quadrupole correlation energy of the configurations with many particles and many holes (np-nh) relative to the normal filling of the spherical mean field orbits (0p-0h). We study the mechanism of mixing between the different configurations, to understand why the super-deformed band survives and how it finally decays into the low-lying spherical states via the indirect mixing of the 0p-0h and 4p-4h configurations.

PACS numbers: 21.10.Sf, 21.60.Cs, 23.20.Lv, 27.40.+z, 29.30.-h

Excited deformed bands in spherical nuclei provide a spectacular example of coexistence of very different structures at the same energy scale, that is a rather peculiar aspect of the dynamics of the atomic nucleus. Several cases are known since long, for instance the four particle four holes and eight particles eight holes states in ^{16}O , starting at 6.05 MeV and 16.75 MeV of excitation energy [1, 2]. However, it is only recently that similar bands, deformed and even super-deformed, have been discovered in other medium-light nuclei such as ^{56}Ni [3], ^{36}Ar [4] and ^{40}Ca [5] and explored up to high spin. These experiments have been possible thanks to the advent of large arrays of γ detectors, like Gammasphere or Euroball. One characteristic feature of these bands is that they belong to rather well defined spherical shell model configurations; for instance, the deformed excited band in ^{56}Ni can be associated with the configuration $(1f_{7/2})^{12}(2p_{3/2}, 1f_{5/2}, 2p_{1/2})^4$ while the (super)deformed bands in ^{36}Ar and ^{40}Ca are based in structures $(sd)^{16}(pf)^4$ and $(sd)^{16}(pf)^8$ respectively. The location of the np-nh states in ^{40}Ca was studied in the Hartree-Fock approximation with blocked particles and Skyrme forces in ref. [6]. While many approaches are available for the microscopic description of these bands (Cranked Nilsson-Strutinsky [4], Hartree-Fock plus BCS with configuration mixing [7], Angular Momentum Projected Generator Coordinate Method [8], Projected Shell Model [9], Cluster models [10] etc.) the interacting shell model is, when affordable, the prime choice. The mean field description of $N=Z$ nuclei, has problems related to the proper treatment of the proton-neutron pairing in its isovector and isoscalar channels. On the shell model side, the problems come from the size of the valence spaces needed to accommodate the np-nh configurations.

In this letter we focus in the ^{36}Ar case, where a rotational band has been experimentally found starting 4.3 MeV above the spherical ground state. It is generated by an intrinsic super-deformed state *i.e.* bearing an axis ratio 2:1. In previous works [4, 11], we have shown

that the experimental super-deformed (SD) band can be associated to the promotion of four particles across the Fermi level, from the *sd* to the *pf* shell. Indeed, this is a very crude description, because the physical states contain components belonging to other np-nh configurations. This mixing allows for transitions connecting the superdeformed band and the low-lying *sd* states. However, the mixing must be gentle enough so as not to jeopardize the very existence of the band. This is the theoretical challenge that we affront in this letter: to explain why the super-deformed band appears at such low excitation energy and how can, at the same time, mix with other configurations and preserve its identity.

Let's recall the results of the calculations at fixed 4p-4h configuration. In the description of the SD band of ^{36}Ar , the natural valence space comprises the *sd* and the *pf* shells. However, the inclusion of the $1d_{5/2}$ orbit produces a huge increase in the size of the basis and massive center of mass effects, forcing us to exclude it from the valence space. The quadrupole coherence of the solutions will be reduced by this truncation. We have quantified the effect and it is moderate as we shall show below. Therefore, our valence space consists of the orbits $2s_{1/2}, 1d_{3/2}, 1f_{7/2}, 2p_{3/2}, 1f_{5/2},$ and $2p_{1/2}$. The basis dimensions are $O(10^7)$. The starting effective interaction is the same used in ref. [4] dubbed SDPF.SM and described in detail in [12]. Blocking the orbit $1d_{5/2}$ minimizes the center of mass contamination of the solutions. Nevertheless, to be safer, we have added to the interaction the center of mass hamiltonian with a small coefficient $\lambda_{cm}=0.5$ to reduce even more unwanted mixings (see [13] for an updated discussion of the center of mass issues). The differences between the results with and without the addition of the center of mass hamiltonian are minor.

In Figure 1 the calculated transition energies are compared with the experimental results in a backbending plot. The agreement is really remarkably good, except at $J=12$ where the data show a clear backbending while the calculation produces a much smoother upbending pat-

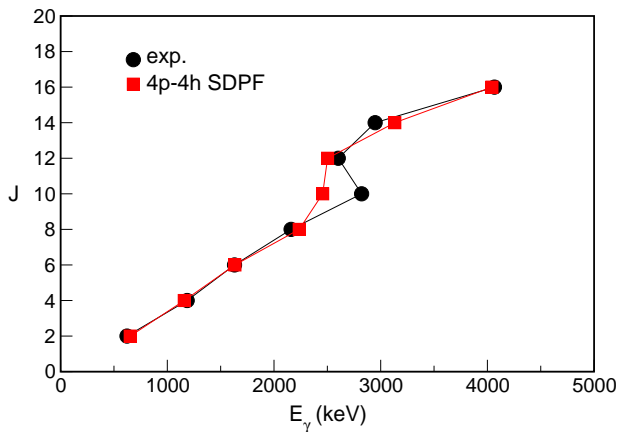


FIG. 1: The superdeformed band in ^{36}Ar ; E_γ 's, exp. vs. 4p-4h calculation

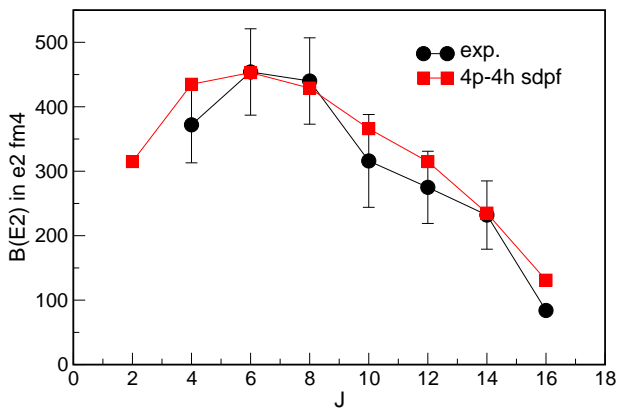


FIG. 2: The superdeformed band in ^{36}Ar ; $B(E2)$'s, exp. vs. 4p-4h calculation. The $J=16$ point is only a lower bound

tern. In the experimental data there is a close-by second 10^+ state, therefore, the discrepancy may be due to the lack of mixing in the calculation. If we move now to Fig. 2 where we gather the experimental [11] and calculated $B(E2)$'s (we use standard effective charges $\delta q_\pi = \delta q_\nu = 0.5$ and $b = 1.94$ fm), we find again an astonishing accord [18]. The value of the intrinsic quadrupole moment corresponds roughly to a deformation $\beta = 0.5$, so that it is justified to speak of a super-deformed band. The origin of such a strong coherence can be attributed to the dominance of Elliott's $SU(3)$ structures in the valence space. The almost perfect agreement achieved by the 4p-4h description, is at the same time a blessing and a challenge. Surprisingly, the incorporation of all the other degrees of freedom must result in essentially no modification at all of the results. And this is not an easy task [19].

The interaction SDPF.SM was originally devised for calculations in fixed $N\hbar\omega$ spaces. In a mixed calculation, some changes must be enforced. In the first place, we must retire from the pairing matrix elements of the pf -

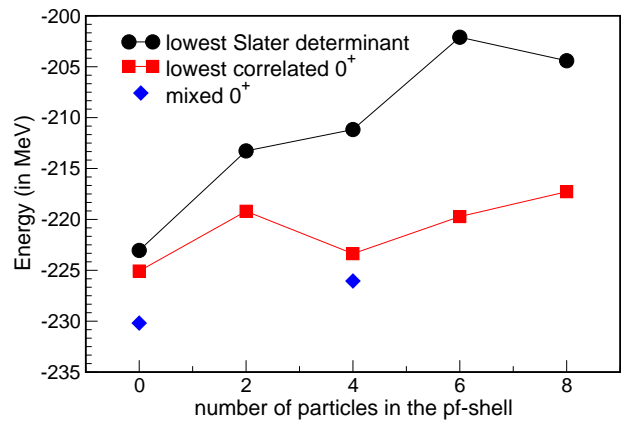


FIG. 3: Relative position of lowest states of the np-nh configurations. Diamonds represent the energies of the ground state and the superdeformed band-head after mixing

shell the implicit effect of the cross shell excitations that now are taken explicitly into account. The amount of this reduction can be estimated in second order perturbation theory to be roughly the square of the off-diagonal matrix element (2 MeV) divided by the gap between the $0p-0h$ and the $2p-2h$ states (8 MeV). We model this effect by reducing all the pf shell $T=1$ pairing matrix elements a 40%. Moreover, the closure of the $1d_{5/2}$ orbit affects differently to the correlation energies of the np-nh configurations and we must correct the calculations for this limitation. To quantify the effect, we have performed calculations in the complete $sd-pf$ space for the $2p-2h$ and $4p-4h$ configurations (in this last case for high- J members of the band). The results show that the $2p-2h$ and $4p-4h$ configurations gain 1.5 MeV and 5.0 MeV more than the $0p-0h$ configuration when the $1d_{5/2}$ orbit is opened. In order to simulate this effect, we have added to the pf -shell monopole interaction a term $\delta\epsilon n_{pf} + 1/2 \delta\bar{V} n_{pf}^{(2)}$, with $\delta\epsilon = -0.5$ MeV and $\delta\bar{V} = -0.5$ MeV. This prescription overestimates the correlation energy of the $8p-8h$ states, but it has no relevant influence in the states we are aiming to. Concerning the $B(E2)$'s, in the case of the $4p-4h$ band, the opening of the $1d_{5/2}$ orbit produces a 12% increase of their values.

Once the interaction has been adapted to the valence space, we proceed to make calculations –using the shell model code ANTOINE [12, 14]– in spaces of fixed np-nh character. Naively one would locate these states at an excitation energy equal to n times the quasi-particle gap between the sd and the pf orbits (~ 7 MeV). In Fig.3 this corresponds to a straight line with slope 7 MeV. This estimation misses two crucial ingredients; first, the presence of quadratic terms in the monopole hamiltonian that can lower substantially the uncorrelated energy of these configurations, and second, the gain in energy of the maximally correlated states within these configurations. To measure the size of the first contribution, we have

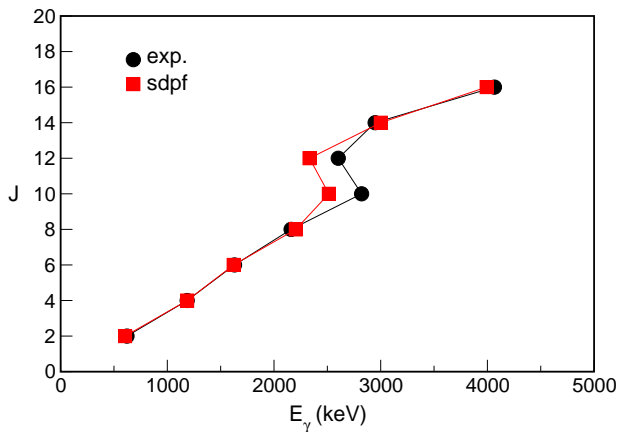


FIG. 4: The superdeformed band in ^{36}Ar ; E_γ 's, comparison with the results of the mixed calculation

computed the energies of the lowest Slater Determinant for each np-nh space. We have plotted them in Fig. 3. Notice that the behavior is not linear; in particular the 4p-4h configuration does not lay 28 MeV above the 0p-0h, but just 12 MeV (see [15] for a fully worked example of this mechanism). The next step is to diagonalize the full interaction in the np-nh spaces to incorporate the correlations at fixed configuration. The results are the squares in Fig. 3 and the correlation energy can be defined as the difference between circles and squares in the figure. The key point is that these correlation energies are very large. In the 4p-4h space, they are large enough to produce a super-deformed rotor whose correlation energy exceeds that of the spherical ground state by 15 MeV, a huge effect that represents 5% of the total binding energy. This suffices to bring the 4p-4h band-head close to degeneracy with the 0p-0h state. It is important to notice that the combined effect of the monopole hamiltonian and the correlation energy favors clearly the 4p-4h super-deformed band which becomes the lowest configuration above the 0p-0h ground state. Both the 2p-2h and the 6p-6h band-heads are higher in energy. This has important consequences for the mechanisms of mixing.

The final step consist in the diagonalization of the interaction in the full valence space. As a consequence of the mixing with the 2p-2h states, the 0p-0h dominated (70%) ground state gains 5 MeV, while the 4p-4h dominated (70%) band-head of the super-deformed band gains 2.5 MeV (see Fig. 3), to finish close to its experimental location (4329 keV exp *vs.* 4319 keV th.). The relative placement of the configurations at fixed np-nh and the intrinsic structure of the np-nh states produce the following very interesting effect: The 4p-4h super-deformed states mix mostly with the 6p-6h ones. A larger mixing with the 2p-2h states would have prompted an earlier and more intense decay-out of the super-deformed band. The 0p-0h and 2p-2h states are of single particle (or spherical nature) and the cross shell pairing interaction *-i.e.* the

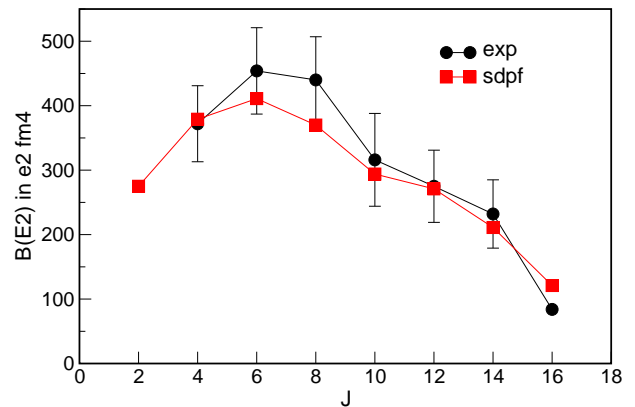


FIG. 5: The superdeformed band in ^{36}Ar ; $B(E2)$'s, exp. vs. mixed results.

scattering of a nuclear Cooper pair from the *sd* to the *pf* shell— mixes them very efficiently. The lower 4p-4h and 6p-6h states are both super-deformed and pairing mixes them too. What turns out to be severely hindered is the mixing of the spherical 2p-2h states with the super-deformed 4p-4h states, as semi-classical arguments suggest. In addition, the states of the super-deformed band cannot decay to those of the 6p-6h band because they lay at higher energies. The decay out of the super-deformed band must then proceed via its small 0p-0h and 2p-2h components.

In Fig. 4 we compare the γ energies along the SD band with the experiment. Even if it seemed difficult to improve upon the agreement of the 4p-4h calculation, the mixed calculation succeeds. Now the backbending is better reproduced while the moment of inertia is still correct. For the first, the interaction of the SD 10^+ with an isolated 2p-2h 10^+ does the job. For the second, the off-diagonal pairing, active in the mixed calculation, compensates the pairing reduction of the effective interaction (as it should). In the range of sensible values of the pairing interaction there is surely room to absorb the hypothetical modifications of the moment of inertia of the SD band due to the opening of the 1d5/2 orbit.

In Fig. 5 we compare the experimental and theoretical $B(E2)$'s through the SD band. The accord is excellent and would become perfect should we increase the calculated values by 12%, the quantity that we have obtained as the effect of the opening of the 1d5/2 in our fragmentary 4p-4h calculations. The reconstruction of the 4p-4h results is due to the fact that the 4p-4h SD states mix with 6p-6h states that are in turn almost as deformed as them. A larger mixing with the (spherical) 2p-2h states would have produced an unwanted reduction of the $B(E2)$'s.

In table I we have gathered the experimental results obtained in [11] for the transitions connecting states of the SD band with other states of the band or 0p-0h or 2p-2h character. The decay-out of the band occurs through the

TABLE I: Out-band transitions in the SD band of ^{36}Ar (B(E2)'s in e^2fm^4 and energies in keV)

	E_γ		B(E2)	
	experiment	theory	experiment	theory
$2_{SD}^+ \rightarrow 0_1^+$	4950	4846	4.6(23)	4.0
$4_{SD}^+ \rightarrow 2_1^+$	4166	3917	2.5(4)	1.2
$4_{SD}^+ \rightarrow 2_2^+$	1697	946	19.2(30)	18.4
$6_{SD}^+ \rightarrow 4_1^+$	3552	2787	5.3(8)	0.25
$10_1^+ \rightarrow 8_{SD}^+$	1975	1192	43.6(74)	13.1
$12_{SD}^+ \rightarrow 10_1^+$	3448	3655	15.0(30)	1.5

transitions $2_{SD}^+ \rightarrow 0_1^+$, $4_{SD}^+ \rightarrow 2_1^+$ and $6_{SD}^+ \rightarrow 4_1^+$, that share two characteristics; a very small transition strength and a large energy release. The calculation reproduces fairly well these properties, thus giving a microscopic explanation of the decay-out. At the bottom of the SD band, the energies of the in-band emitted γ 's become small, and the phase space enhancement of the transitions to the low lying spherical states compensates the smallness of the transition strengths. In the upper part of the band, the presence of a 2p-2h 10^+ yrast state. produces a weak out-band excursion that is also well given by the calculation.

The mean field calculation of ref. [7] is possibly the closest to ours. Albeit it is limited to the low spin regime $J \leq 6$, it incorporates the mixing of different projected mean field solutions using the Generator Coordinate Method. As we have mentioned before, the standard mean field calculations do not treat properly the proton neutron pairing. In the cranking approximation this results in a too large moment of inertia. Indeed, as shown for the ^{48}Cr case in ref. [16], the correct treatment of the neutron proton pairing halves the moment of inertia. Paradoxically, the moments of inertia of the SD bands calculated in [7] are too small. According to the authors this is a drawback of their method, related to absence of $\Delta K=0$ admixtures, as discussed in [17]. This spurious reduction of the moment of inertia overcompensates the effect of their bad treatment of the proton neutron pairing. The cancellation of this two –unphysical– but opposite contributions can eventually produce an unwanted “correct” moment of inertia. As pointed out by the authors of ref. [8], this is actually the case in their AMP-CGM calculation using the Gogny force. The in-band B(E2)'s of the SD band are clearly overestimated in [7] while for the transitions out of the band their predictions are acceptable but less accurate than ours.

To complete the description we have calculated a side band of negative parity with a 3^- band-head at 4178 keV, $E_\gamma(5^- \rightarrow 3^-) = 993$ keV and $E_\gamma(6^- \rightarrow 5^-) = 2183$ keV also reported in [11]. In order to describe the negative parity states we find that it is compulsory to open the $1d_{5/2}$ orbit. As a full calculation is out of reach, we have computed the negative parity states in the space

of the 1p-1h and 3p-3h configurations, referring them to the ground state energy calculated in the space of the 0p-0h and 2p-2h configurations. The results are reasonable with the 3^- at 5040 keV, $E_\gamma(5^- \rightarrow 3^-) = 751$ keV and $E_\gamma(6^- \rightarrow 5^-) = 2010$ keV. Notice that ^{36}Ar exhibits at around 4 MeV a multiplet of nearly degenerate states of 0p-0h, 1p-1h and 4p-4h nature, that the calculations are able to explain simultaneously.

In conclusion, we have shown that “state of the art” shell model calculations in the valence space spanned by two major oscillator shells can provide a unified description of many coexisting nuclear structures; spherical states of single particle nature, negative parity states of octupole character and a super-deformed band built on 4p-4h excitations. In particular, we have shown why the super-deformed band appears at such a low excitation energy and how the indirect mixing of very different states governs the decay-out of the super-deformed band.

This work is partly supported by the IN2P3(France) CICYT(Spain) collaboration agreements. AP's work is supported by MCyT (Spain), grant BFM2003-1153.

-
- [1] E. B. Carter, G. E. Mitchell and R. H. Davis, Phys. Rev. **133** 1421 (1964).
 - [2] P. Chevallier, F. Scheibling, G. Goldring, I. Plessner and M. W. Sachs, Phys. Rev. **160** 827 (1967).
 - [3] D. Rudolph, *et al.*, Phys. Rev. Lett. **82**, 3763 (1999).
 - [4] C. E. Svensson, *et al.*, Phys. Rev. Lett. **85**, 2693 (2000).
 - [5] E. Ideguchi, *et al.*, Phys. Rev. Lett. **87**, 222501 (2001).
 - [6] D. C. Zheng, L. Zamick and D. Berdichevsky, Phys. Rev. C **38**, 437 (1988).
 - [7] M. Bender, H. Flocard and P.-H. Heenen, Phys. Rev. C **68**, 044321 (2003).
 - [8] R. R. Rodríguez-Guzmán, J. L. Egido and L. M. Robledo, Intl. J. of Mod. Phys. **E13**, 139 (2004)
 - [9] G.-L. Long and Y. Sun, Phys. Rev. C **63**, 021305 (2001).
 - [10] T. Sakuda and S. Ohkubo, Nucl. Phys. **A744** 77 (2004).
 - [11] C. E. Svensson, *et al.*, Phys. Rev. C **63**, 061301(R) (2001).
 - [12] E. Caurier *et al.*, arXiv/nucl-th/0402046, Rev. Mod. Phys. (in press).
 - [13] D. Dean *et al.*, Phys. Rev. C **59**, 2474 (1999).
 - [14] E. Caurier, ANTOINE code, Strasbourg (1989-2002. . .).
 - [15] A.P. Zuker in “Contemporary Nuclear Shell Models” X. Pang, D. H. Feng and M. Vallieres eds. Lecture Notes in Physics, vol 482, pag. 93, Springer 1997.
 - [16] E. Caurier *et al.*, Phys. Rev. Lett. **75** 2466 (1995).
 - [17] R. R. Rodríguez-Guzmán, J. L. Egido and L. M. Robledo, Phys. Rev. C **62**, 054219 (2000)
 - [18] Actually it can be seen to be better than it was in [11]. The reason is that there, the default value of the oscillator size parameter in the codes; $b=1.01 \text{ A}^{1/6} \text{ fm}$, which is a 5% smaller than the correct one for these light nuclei, was inadvertently used.
 - [19] As the Queen says to the protagonist of “Alice through the looking glass”: “Now, here, you see, it takes all the *running* you can do to keep in the same place . . .”